

6th International Conference on Silicon Photovoltaics, SiliconPV 2016

Boron-Oxygen defect formation rates and activity at elevated temperatures

Phillip Hamer^{a,b}, Nitin Nampalli^b, Ziv Hameiri^b, Moonyong Kim^b, Daniel Chen^b,
Nicholas Gorman^b, Brett Hallam^b, Malcolm Abbott^b, Stuart Wenham^b

^aThe University of Oxford, Department of Materials, 16 Parks Rd, Oxford, OX1 3PH, United Kingdom

^bThe University of New South Wales, School of Photovoltaics and Renewable Energy Engineering, Tyree Energy Technology Building, UNSW, Sydney, 2052, NSW, Australia

Abstract

In this work the dependence of the slow boron-oxygen defect formation rate on excess carrier density is examined in p-type Cz silicon. In order to examine behavior at elevated temperatures simple models are developed to simulate the injection-level dependent lifetime of samples at a range of temperatures and active defect concentrations. These models are then verified against experimental data. Based on these models it is possible to clearly observe a quadratic dependence of defect formation rate upon total hole concentration over a range of temperatures. The implications of a hole (and hence excess carrier (Δn)) dependent defect formation rate, combined with the temperature dependence of defect activity are then discussed. It is demonstrated how a dependence of formation rate upon hole concentration increases the rate of defect formation and mitigation of carrier-induced degradation in samples with reduced saturation current density during anneals at elevated temperatures and illumination intensities.

© 2016 The Authors. Published by Elsevier Ltd.

Peer review by the scientific conference committee of SiliconPV 2016 under responsibility of PSE AG.

Keywords: Boron-oxygen; Degradation; Passivation; Defect Kinetics; Crystalline silicon

1. Introduction

The boron oxygen (BO) defect has been of significant interest to the photovoltaic community for over a decade [1]. While there is still some debate as to the exact form of the defect, it has been shown to be responsible for decreases in efficiency of as much as 2% absolute for cells fabricated on boron-doped Czochralski (Cz) silicon. A method of permanently mitigating the effects of the defect was reported by Herguth *et al.* in 2006 [2]. There has been significant recent research activity focused upon the acceleration of this process for industrial devices [3].

This study uses a three-state model for the boron oxygen defect [2, 4, 5]. The inactive state is the most common form after high temperature processing and has very little effect on recombination. During a defect formation process, which involves carrier injection at temperatures below 443 K, the defects transition to the active state which greatly increases recombination in the wafer. A defect passivation process transitions defects from the active state to the passivated (or regenerated) state, which does not degrade under low temperature illumination. A transition from the passivated to the active state will be referred to as de-stabilization while transition from the active to inactive state will be referred to as dissociation.

1.1. Acceleration of BO defect formation rate

The formation of the BO defect has been observed to consist of two elements, a fast and a slow defect formation process [6, 7]. It is the slow defect formation process that ultimately limits device performance and mitigation of the defect. This paper deals solely with the slow process and will henceforth refer to this process as defect formation. The fast process was not observed as it occurs almost instantaneously at the elevated temperatures and illumination intensities used.

It has been shown that the defect formation rate can be greatly enhanced in *p*-type silicon under high intensity illumination [8, 9]. This is in apparent contradiction with previous results where the defect formation rate appeared to plateau for illumination intensities in excess of 0.1 Suns [6, 10, 11]. It is possible to resolve this contradiction if a dependence of the defect formation rate upon the hole concentration is considered. A number of studies have observed a dependence of the formation rate upon equilibrium hole concentration [6, 12, 13], under conditions where the excess carrier density is significantly lower than the equilibrium hole concentration, and where it is therefore difficult to distinguish between a dependence upon the equilibrium concentration, p_0 , and the total concentration $p = p_0 + \Delta n$.

A dependence of defect formation rate on either of pp_0 or p^2 would reflect the enhancement of the defect formation rate under medium to high injection levels while remaining in agreement with previous observations at lower injections. Of these two possibilities, recent observations in compensated *n*-type silicon [14, 15] would appear to support a quadratic, rather than linear, dependence of the defect formation rate upon the total hole concentration.

1.2. Importance of defect formation rate for defect mitigation

The defect formation rate is of critical importance to the rapid mitigation of the BO defect. There is significant evidence that in order for the defects to be passivated, such that they do not subsequently become active, they must first be formed [4, 16]. At low temperatures defect formation is generally more rapid than defect passivation, however at temperatures above 473 K the defect formation rate is substantially lower than the defect passivation rate, to the extent that it dominates the total process time [5].

Fig. 1 presents the normalized defect densities (NDD) after light soaking, which is proportional to the number of defects *not* in the passivated state, for samples annealed at high temperatures with a high photon flux. The simulations in the figure demonstrate how increased defect formation rates increase both the rate of defect mitigation at temperatures between 450–600 K, as well as the temperature at which effective defect mitigation is possible [4].

In this paper a quadratic dependence of the slow BO defect formation rate upon p will be demonstrated, and therefore how it may be greatly accelerated with sufficient generation of excess carriers. It will also be shown that due to this strong excess carrier dependence the recombination within the device, and in particular in the near-surface regions, can greatly alter the ability to form and subsequently passivate the defect during rapid mitigation processes at temperatures above 473 K with high intensity illumination.

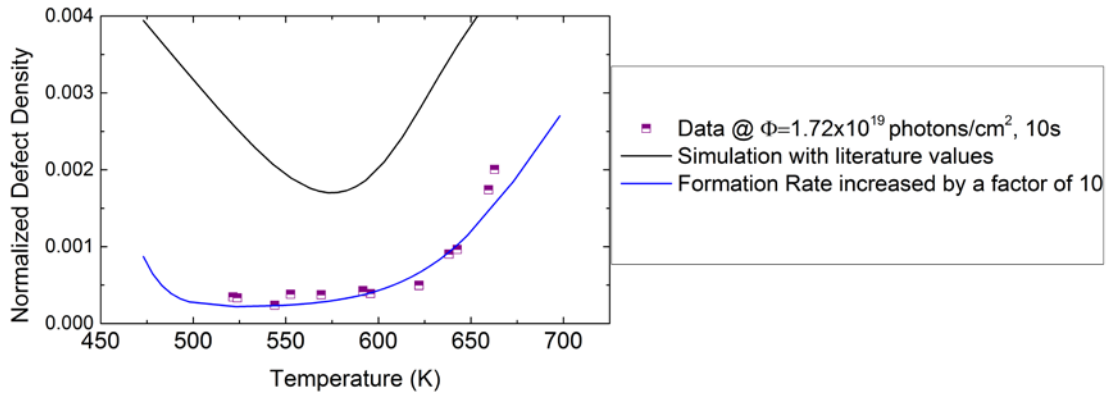


Fig. 1. Observed active normalized defect densities after 48 h light soaking for a 10 s process with a photon flux of 1.7×10^{19} photons/cm² after [4]. Simulations are also presented using standard values in the literature [6, 17], as well as for accelerated passivation rates.

2. Experimental method

2.1. Sample preparation

Test structures were prepared using commercial grade 156 mm × 156 mm boron-doped Cz wafers ($1.73 \Omega\text{cm}$, $N_A = 8.4 \times 10^{15} \text{ cm}^{-3}$). The substrates were subjected to alkaline texturing, with a resultant total wafer thickness of approximately 180 μm . This was followed by an RCA clean and HF dip; phosphorous diffusions were then carried out in a tube furnace to produce a range of different sheet resistances (40–250 Ω/\square), that resulted with different saturation current densities J_0 (40–400 fA/cm^2). Subsequently, hydrogenated silicon nitride ($\text{SiN}_x\text{:H}$) with a refractive index of 2.08 (measured at 633 nm) was deposited onto both surfaces of the wafers using a plasma-enhanced chemical vapour deposition (PECVD) system. Where it was desired to observe defect passivation, wafers were annealed in a fast-firing belt furnace with a peak set point temperature of 700 °C for several seconds to release hydrogen from the dielectric and distribute it throughout the silicon bulk (fired) [18]. For substrates where only the defect formation was of interest, the wafers were not fired in order to suppress any passivation (unfired).

The defects were then transitioned into the desired states for the experiments. Where it was required that the defects be in the inactive state, a standard dark annealing process was used. This process consisted of heating the samples on a hotplate at 503 K for 10 min without illumination. If instead the defects needed to be in the active state, a temperature controlled light soaking process was used [19]. This conventional degradation process was performed under a halogen lamp with an irradiance of $78 \pm 1 \text{ mW/cm}^2/\text{s}$ with wafers maintained at a temperature of $313 \pm 3 \text{ K}$ for 48 h.

Processing was performed on a hotplate under 938 nm laser illumination. The laser was operated in quasi-continuous wave mode with a pulse length of 0.5 ms and repetition frequency of 2 kHz. A beam shaper was used to enable illumination of the entire sample, and intensities ranging from 5×10^{17} photons/cm²/s to 2×10^{19} photons/cm²/s were achieved by varying the laser power and/or expansion of the beam. Samples were removed from the hotplate and rapidly cooled upon completion of the laser process. The substrate temperature was measured in situ using a Calex pyrocouple (PC301HT-0) infrared thermometer, sensing radiation wavelengths between 8 μm and 14 μm . The output was logged using a high speed logger (USB-4704-AE), sampling at 100 ms intervals. The output voltage was then calibrated using a contact thermocouple without illumination.

After processing, the samples were once again light soaked in order to determine the stabilized lifetimes, which in turn allowed observation of the passivated concentrations of the defect.

Effective minority carrier lifetimes (τ_{eff}) as a function of Δn were measured after each process step using a WCT-120 (Sinton Instruments) photoconductance lifetime tester [20]. The measured data was analysed using the generalized technique [21]. Where relevant, lifetimes were extracted at a single Δn of $8.4 \times 10^{14} \text{ cm}^{-3}$, equivalent to $0.1 \times N_A$, where N_A is the bulk doping concentration.

NDD were calculated from these extracted lifetimes and from the extracted lifetimes after dark annealing (DA) as [22]:

$$NDD = \frac{1}{\tau_{eff}} - \frac{1}{\tau_{eff_DA}} \quad (1)$$

From the NDD, fractional defect densities (FDD) were calculated using the dark annealed and light soaked lifetimes:

$$FDD = \frac{NDD}{NDD_{LS}} \quad (2)$$

where NDD_{LS} is the NDD measured after light soaking.

2.2. Sample lifetime at elevated temperatures

In order to establish the dependence of the defect formation rate on p , the hole concentration needs to be determined as a function of both the illumination intensity and the temperature used during the defect formation process. In addition, most recovery processes for carrier induced degradation are carried out at elevated temperatures, and it is therefore important to investigate the carrier lifetimes under these conditions.

A Sinton Instruments WCT-120TS was used to measure the injection level dependent lifetimes of samples between 300–453 K. These measurements were used to develop a simple model for the purposes of evaluating hole concentrations under medium to high injection, based on a fixed bulk lifetime τ_{bulk} and J_0 was found to be sufficient. The lifetime was then modelled as:

$$\frac{1}{\tau_{eff}(\Delta n)} = \frac{1}{\tau_i} + \frac{1}{\tau_{bulk}(T)} + \frac{2J_0(T)(p+\Delta n)}{qwn_i^2} \quad (3)$$

where the intrinsic lifetime τ_i was modelled using the temperature dependent ambipolar Auger coefficient of Wang and Macdonald [23], w is the sample thickness in cm and n_i is the intrinsic carrier concentration.

Fig. 2 presents Arrhenius plots for extracted J_0 and τ_{bulk} from lifetime samples using the Kane-Swanson method where the defects are in the inactive state [24]. The significant increase of J_0 with temperature can be completely explained by the strong dependency of n_i on temperature [25, 26]. As expected, τ_{bulk} also increases with increased temperature; the rate of the improvement is impacted by both the energy level of the defect and the temperature-dependence of the capture cross section ratio [27]. The activation energy for this increase was found to be 0.084 eV, which is in good agreement with previous observations of the activity of the BO defect in its inactive state [28].

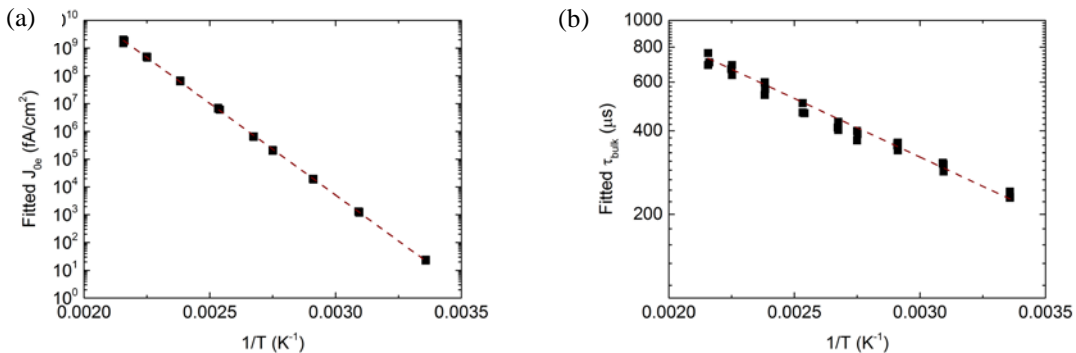


Fig. 2. Arrhenius plots of fitted J_0 (a) and τ_{bulk} (b) for 1.7 Ω .cm p -type Cz lifetime samples

The simulated lifetimes modelled using these relations are compared with measurements at temperatures ranging from 353–453 K in Fig. 3. A good fit is observed for injection levels above $2 \times 10^{15} \text{ cm}^{-3}$ for the J_0 values used in these experiments. At lower injection levels, the samples with lower J_0 show significant deviation due to asymmetric SRH recombination and shunting effects. However, these injection levels are of limited interest for rapid defect mitigation since p is not greatly altered. Furthermore, the error introduced in the simulated Δn at low injection conditions does not greatly affect the estimation of p .

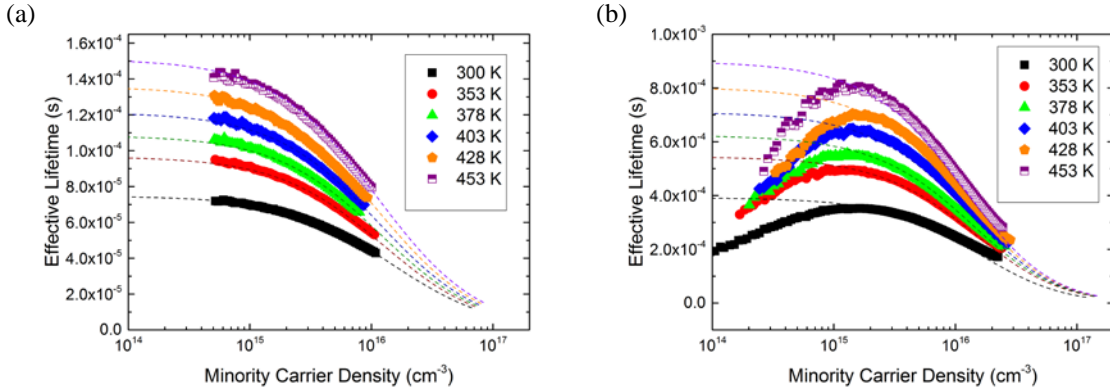


Fig. 3. Simulated and measured effective lifetimes as a function of minority carrier density at various temperatures for $J_0 = 173 \text{ fA/cm}^2$ (a) and $J_0 = 24 \text{ fA/cm}^2$ (b).

The observed behavior for J_0 can readily be extended to the case where the defects are in the active state is more complex, as shown in Fig. 4. At low temperatures a similar trend is observed as for the inactive case, however at higher temperatures the fitted bulk lifetime begins to increase rapidly with temperature as observed by Glunz *et al.* [28]. In order to fit these curves a more involved consideration of the asymmetric SRH recombination activity would be required.

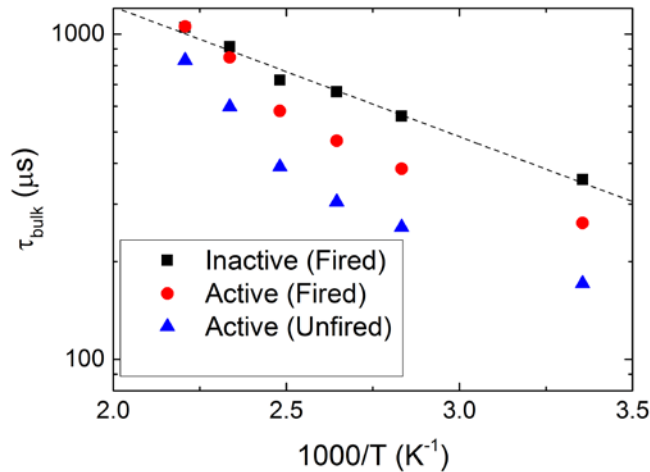


Fig. 4. Extracted bulk lifetimes for wafers with a J_0 of between $40\text{--}50 \text{ fA/cm}^2$ with wafers in the active or inactive states.

The simple models described in this section were used to estimate the injection level dependent lifetime, and hence Δn of samples at a range of temperatures and photon fluxes throughout this study.

3. Results

3.1. Observation of defect formation rate

In order to observe the dependence of BO defect formation rate on unfired samples were processed at temperatures between 374–417 K under a range of illumination intensities. The calculated fraction of active defects in lifetime samples after annealing for various photon fluxes are presented in Fig. 5. Data fitting was performed with a simple model including both defect formation and dissociation and a constant defect formation rate throughout the process [5]. The influence of the fast defect formation process was accounted for by an offset in the initial defect concentration. This offset was a uniform 13% of the saturated defect concentration in all cases. The resulting defect formation rates can be found in Table 1.

The use of a constant defect formation rate is clearly not ideal, and introduces some error in situations where the majority of defects are in the active state. Under these conditions the bulk lifetime of the samples is reduced, which should in turn reduce Δn and hence the formation rate. These errors were considered acceptable under current conditions as the fitting is more strongly influenced by the results at the shortest time steps.

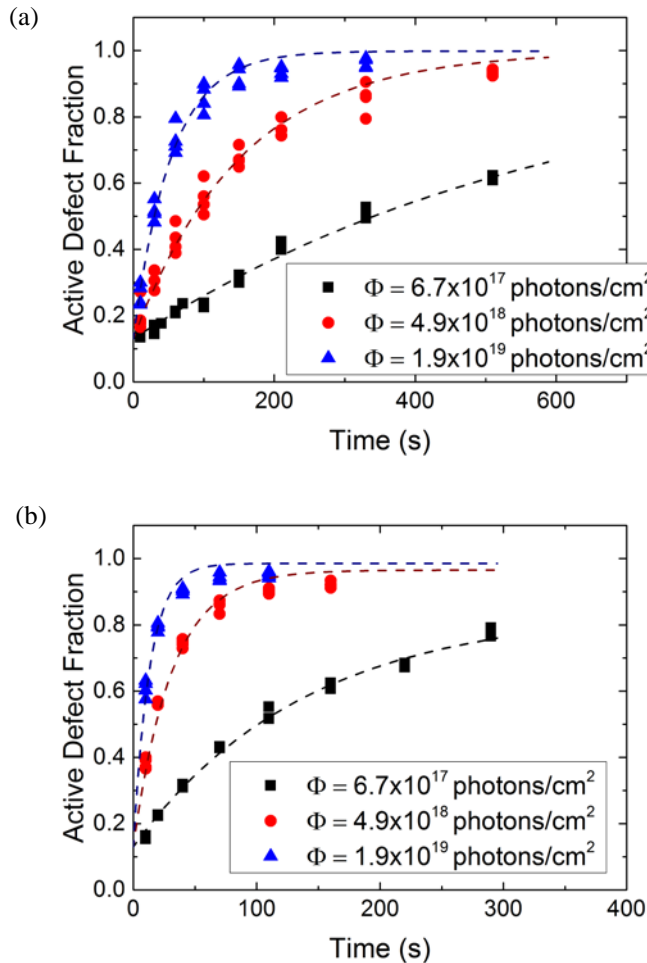


Fig. 5. Active defect fractions of unfired wafers after annealing processes under photon fluxes between 6.7×10^{17} – 1.9×10^{19} photons/cm² for a temperature of 374 K (a) and 417 K (b). The dashed lines represent fits to the data using a constant defect formation rate.

Table 1. Extracted defect formation rates (s^{-1}) for a range of temperatures and photon fluxes

Photon Flux (photons/cm ²)	374 K	393 K	417 K
6.7×10^{17}	1.67×10^{-3}	3.65×10^{-3}	6.09×10^{-3}
4.9×10^{18}	6.56×10^{-3}	1.46×10^{-2}	3.18×10^{-2}
1.9×10^{19}	1.86×10^{-2}	3.40×10^{-2}	7.36×10^{-2}

It was not possible to obtain a reasonable fit for the data in Table 1 using a linear relationship between p and the defect formation rate. In contrast, an excellent fit is obtained using a quadratic relationship, as depicted in Fig. 6. Furthermore, when the quadratic pre-factors were plotted on an Arrhenius graph, an activation energy E_A of 0.415 ± 0.02 eV was obtained, which is within the range of the estimated activation energy for defect formation [6, 10, 29]. It is therefore concluded that the formation rate of the BO defect has a quadratic dependence upon p at medium to high injection levels in p -type silicon and may be expressed as:

$$R_{\text{formation}} = Cp^2 e^{\frac{-E_A}{kT}} \quad (4)$$

where C is a carrier concentration and temperature independent pre-factor under these conditions in p -type silicon. It may readily be observed that this expression is not a sufficient description at low injection levels, since defect formation is not observed without carrier injection. Investigation is ongoing into developing a model that explains both the low and high injection behaviour.

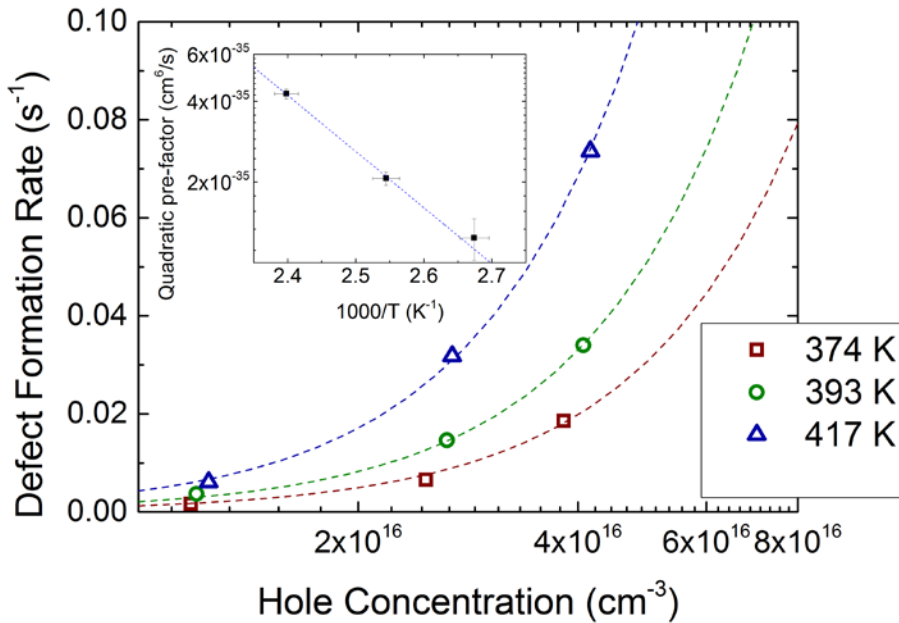


Fig. 6. Fitted defect formation rates as a function of calculated hole concentration for temperatures between 374–417 K and (inset) Arrhenius plot for temperatures between 374–417 K.

3.2. Importance of J_0 for defect formation and mitigation

A quadratic dependence implies that the defect formation rate may be significantly enhanced when Δn in excess of the bulk doping concentration are realized. In order to both, form and passivate the defect as quickly as possible, it is also advantageous to use temperatures in excess of 473 K [3, 4]. In Section 2.2 it was observed that τ_{bulk}

increases rapidly with increasing temperature and bulk recombination is unlikely to be a significant component of the total at these temperatures and excess carrier concentrations. The injection level dependent lifetime will instead be dominated by the J_0 term and, at the highest injection levels, Auger recombination. It would therefore be predicted that under identical conditions defect formation, and hence rapid defect mitigation techniques, should be enhanced in samples with low J_0 .

Fig 7 below presents the active defect formation for un-fired wafers with different J_0 values as a function of time when annealed at 380 K under a photon flux of 1.04×10^{19} photons/cm². Due to the different effective lifetimes of the samples under injection the excess carrier densities, and hence hole concentrations, decrease with increasing J_0 . The calculated hole concentrations in these samples were used to predict a defect formation rate using equation 5, as well as the pre-factor and activation energy from Fig. 6. It may clearly be seen that there is reasonable agreement between the experimental results and this simple model based on quadratic dependence. However the inaccuracy of using a single defect formation rate throughout the process is clearly visible in the fit to the samples with the lowest J_0 .

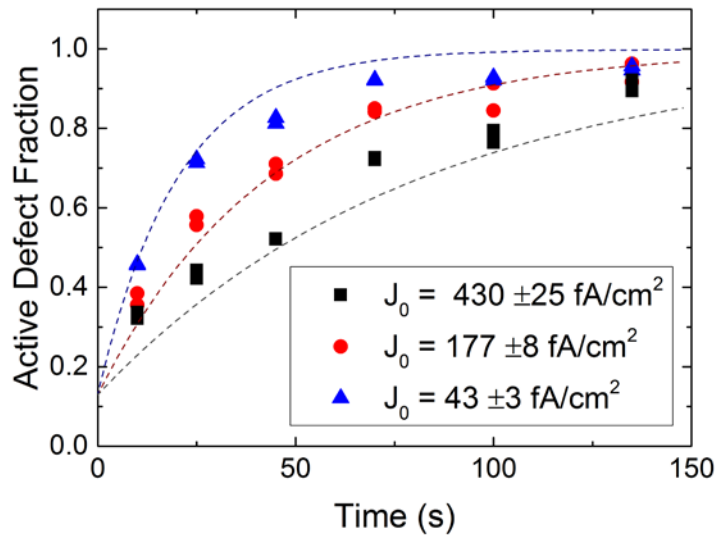


Fig. 7. Active defect fractions of unfired wafers after annealing processes for J_0 between 40–455 fA/cm² with a photon flux of 1.09×10^{19} photons/cm² at a temperature of 374 K. The lines present simulations using the calculated hole concentrations and the activation energy and pre-factor determined from the results in Fig. 6.

If defect formation is increased, it is possible to increase the speed at which defects transition from the inactive to the passivated state. It has been observed that when fired samples are annealed at temperatures above 433 K, that if the defects are initially in the inactive state the number of defects passivated as a function of time is initially much smaller than if the defects are initially in the active state [4]. This is explained by the requirement for the defect to be in the active state before it can be passivated. Fig. 8 presents results for fired wafers where the defects began the anneals with defects in the inactive state. Again it is clear that the process has been accelerated for samples with lower J_0 values, in reasonable agreement with the model developed in section 3.1. In this case the difference between the simulated results and the experimental values is largely influenced by the values used for the rate of other reactions for the BO defect.

4. Summary and conclusions

The dependence of the formation rate of the BO defect on the hole concentration was investigated. It was observed that experimental results on *p*-type silicon under medium to high injection conditions could be fitted using a quadratic dependence. The consequence of such a dependence is that the recombination activity within the wafer will have a significant impact upon the ability to form, and hence mitigate, the BO defect.

Recombination activity of the BO defect itself is likely to have a very limited impact on rapid mitigation approaches [4, 30] at temperatures in excess of 473 K. At these temperatures, recombination due to the deep donor level of the defect is negligible. In addition, the active concentration at any time during these processes is typically very small.

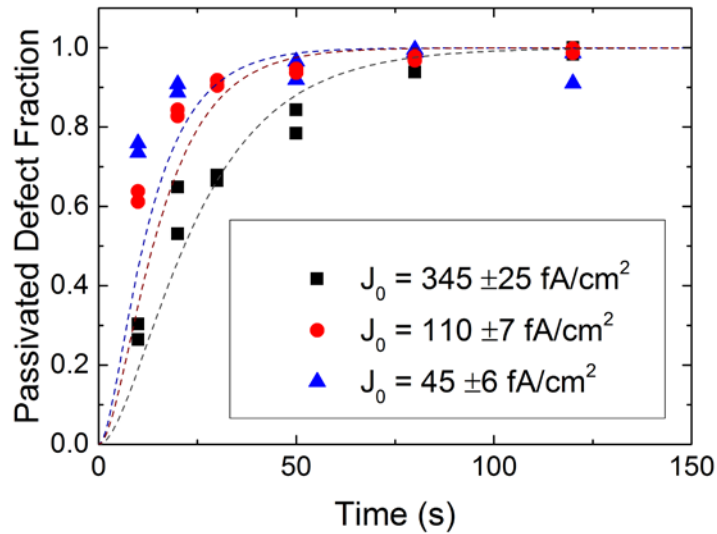


Fig. 8. Passivated defect fractions of fired wafers as a function of time for J_0 values between 40–360 fA/cm² after annealing with a photon flux of 6.6×10^{18} photons/cm² at 445 K. Samples began the process with all defects in the inactive state. The lines present simulations using the calculated hole concentrations and the activation energy and pre-factor determined from the results in FIG 6, along with values for defect passivation and de-stabilization from Wilking *et al.* [3].

In contrast, recombination at surfaces and near surface regions such as emitters that contribute to J_0 greatly affect the effective lifetime of samples during rapid mitigation techniques at elevated temperatures and illumination intensities. It has been demonstrated that when defects begin a process in the inactive state the rate at which they can be transitioned to the passivated state is enhanced in samples with low J_0 . This would indicate that cell architectures with reduced sources of such recombination, such as PERC cells, could allow more rapid passivation of the BO defect after firing.

5. Acknowledgements

This study has been supported by the Australian Government through the Australian Renewable Energy Agency (ARENA 1-060 and ARENA 2014/RND097) and the Australian Centre for Advanced Photovoltaics (ACAP PP1.1). The views expressed herein are not necessarily the views of the Australian Government, and the Australian Government does not accept responsibility for any information or advice contained herein. The authors would like to thank the commercial partners of the ARENA 1-060 advanced hydrogenation project, as well as Ly Mai and Nino Borojevic for assisting with sample fabrication. PH would like to acknowledge funding from the EPSRC

Supersilicon (Grant EP/M024911/1), while ZH acknowledges the support of the Australian Research Council (ARC) through the Discovery Early Career Researcher Award (DECRA, Project DE150100268).

References

- [1] J. Schmidt, K. Bothe, Structure and transformation of the metastable boron- and oxygen-related defect center in crystalline silicon, *Physical Review B*, 69 (2004) 024107.
- [2] A. Herguth, G. Schubert, M. Kaes, G. Hahn, A new approach to prevent the negative impact of the metastable defect in boron doped cz silicon solar cells, in: *Photovoltaic Energy Conversion, Conference Record of the 2006 IEEE 4th World Conference on*, IEEE, 2006, pp. 940-943.
- [3] S. Wilking, M. Forster, A. Herguth, G. Hahn, From simulation to experiment: Understanding BO-regeneration kinetics, *Solar Energy Materials and Solar Cells*, 142 (2015) 87-91.
- [4] P. Hamer, B. Hallam, M. Abbott, C. Chan, N. Nampalli, S. Wenham, Investigations on accelerated processes for the boron–oxygen defect in p-type Czochralski silicon, *Solar Energy Materials and Solar Cells*, 145 (2016) 440-446.
- [5] B. Hallam, M. Abbott, N. Nampalli, P. Hamer, S. Wenham, Implications of Accelerated Recombination-Active Defect Complex Formation for Mitigating Carrier-Induced Degradation in Silicon, *IEEE Journal of Photovoltaics*, 6 (2016) 92-99.
- [6] K. Bothe, J. Schmidt, Electronically activated boron-oxygen-related recombination centers in crystalline silicon, *Journal of Applied Physics*, 99 (2006) 013701-013711.
- [7] T. Naeerland, H. Angelskär, E. Marstein, Direct monitoring of minority carrier density during light induced degradation in Czochralski silicon by photoluminescence imaging, *Journal of Applied Physics*, 113 (2013) 193707.
- [8] P. Hamer, B. Hallam, M. Abbott, S. Wenham, Accelerated formation of the boron–oxygen complex in p-type Czochralski silicon, *physica status solidi (RRL) – Rapid Research Letters*, 9 (2015) 297-300.
- [9] T. Schutz-Kuchly, S. Dubois, J. Veirman, Y. Veschetti, D. Heslinga, O. Palais, Light-induced degradation in compensated n-type Czochralski silicon solar cells, *physica status solidi (a)*, 208 (2011) 572-575.
- [10] D. Palmer, K. Bothe, J. Schmidt, Kinetics of the electronically stimulated formation of a boron-oxygen complex in crystalline silicon, *Physical Review B*, 76 (2007) 035210.
- [11] J. Schmidt, K. Bothe, R. Hezel, Formation and annihilation of the metastable defect in boron-doped Czochralski silicon, in: *Photovoltaic Specialists Conference, 2002. Conference Record of the Twenty-Ninth IEEE, 2002*, pp. 178-181.
- [12] D. Macdonald, A. Liu, A. Cuevas, B. Lim, J. Schmidt, The impact of dopant compensation on the boron–oxygen defect in p- and n-type crystalline silicon, *physica status solidi (a)*, 208 (2011) 559-563.
- [13] B. Lim, F. Rougieux, D. Macdonald, K. Bothe, J. Schmidt, Generation and annihilation of boron–oxygen-related recombination centers in compensated p-and n-type silicon, *Journal of Applied Physics*, 108 (2010) 103722-103722-103729.
- [14] T. Niewelt, J. Schön, J. Broisch, S. Rein, J. Haunschild, W. Warta, M.C. Schubert, Experimental Proof of the Slow Light-Induced Degradation Component in Compensated n-Type Silicon, in: *Solid State Phenomena, Trans Tech Publ*, 2015, pp. 102-108.
- [15] J. Schön, T. Niewelt, J. Broisch, W. Warta, M.C. Schubert, Characterization and modelling of the boron-oxygen defect activation in compensated n-type silicon, *Journal of Applied Physics*, 118 (2015) 245702.
- [16] A. Herguth, G. Hahn, Kinetics of the boron-oxygen related defect in theory and experiment, *Journal of Applied Physics*, 108 (2010) 114509.
- [17] S. Wilking, C. Beckh, S. Ebert, A. Herguth, G. Hahn, Influence of bound hydrogen states on BO-regeneration kinetics and consequences for high-speed regeneration processes, *Solar Energy Materials and Solar Cells*, 131 (2014) 2-8.
- [18] N. Nampalli, B. Hallam, C. Chan, M. Abbott, S. Wenham, Evidence for the role of hydrogen in the stabilization of minority carrier lifetime in boron-doped Czochralski silicon, *Applied Physics Letters*, 106 (2015) 173501.
- [19] J. Schmidt, K. Bothe, and R. Hezel. Formation and annihilation of the metastable defect in boron-doped Czochralski silicon. in *Photovoltaic Specialists Conference, 2002. Conference Record of the Twenty-Ninth IEEE. 2002*.
- [20] R. Sinton and A. Cuevas, Contactless determination of current–voltage characteristics and minority-carrier lifetimes in semiconductors from quasi-steady-state photoconductance data. *Applied Physics Letters*, 1996. 69(17): p. 2510-2512.
- [21] H. Nagel, C. Berge, and A. Aberle, Generalized analysis of quasi-steady-state and quasi-transient measurements of carrier lifetimes in semiconductors. *Journal of Applied Physics*, 1999. 86(11): p. 6218-6221.
- [22] S. Rein, T. Rehrl, W. Warta, S. Glunz, G. Willeke,. Electrical and thermal properties of the metastable defect in boron-doped Czochralski silicon (Cz-Si). in *Proceedings of the 17th European Photovoltaic Solar Energy Conference. 2001*.
- [23] S. Wang, D. Macdonald, Temperature dependence of Auger recombination in highly injected crystalline silicon, *Journal of Applied Physics*, 112 (2012) 113708.
- [24] D. Kane, R. Swanson, Measurement of the emitter saturation current by a contactless photoconductivity decay method, in: *IEEE photovoltaic specialists conference. 18, 1985*, pp. 578-583.
- [25] K. Misiakos, D. Tsamakis, Accurate measurements of the silicon intrinsic carrier density from 78 to 340 K, *Journal of Applied Physics*, 74 (1993) 3293-3297.
- [26] P. Altermatt, A. Schenk, F. Geelhaar, G. Heiser, Reassessment of the intrinsic carrier density in crystalline silicon in view of band-gap narrowing, *Journal of Applied Physics*, 93 (2003) 1598-1604.
- [27] S. Rein, *Lifetime Spectroscopy: A Method of Defect Characterization in Silicon for Photovoltaic Applications*, Springer, 2005.
- [28] S. Glunz, S. Rein, J. Lee, W. Warta, Minority carrier lifetime degradation in boron-doped Czochralski silicon, *Journal of Applied Physics*, 90 (2001) 2397-2404.

- [29] B. Lim, F. Rougieux, D. Macdonald, K. Bothe, J. Schmidt, Generation and annihilation of boron–oxygen-related recombination centers in compensated p- and n-type silicon, *Journal of Applied Physics*, 108 (2010) 103722.
- [30] S. Wilking, S. Ebert, C. Beckh, A. Herguth, G. Hahn, High Speed Regeneration of BO-Defects: Improving Long-Term Solar Cell Performance within Seconds, in: *The 29th European PV Solar Energy Conference and Exhibition*, Amsterdam, 2014.